HHS Public Access

Author manuscript

Free Radic Biol Med. Author manuscript; available in PMC 2021 February 20.

Published in final edited form as:

Free Radic Biol Med. 2020 February 20; 148: 70–82. doi:10.1016/j.freeradbiomed.2019.12.037.

Fumarate and Oxidative Stress Synergize to Promote Stability of C/EBP Homologous Protein in the Adipocyte

Allison M. Manuel[a], **Michael D. Walla**[b], **Margaret Dorn**[a], **Ross M. Tanis**[a], **Gerardo G. Piroli**[a], **Norma Frizzell**[a,*]

[a]Department of Pharmacology, Physiology & Neuroscience, School of Medicine, University of South Carolina, Columbia, SC 29209, USA

[b]Mass Spectrometry Center, Department of Chemistry & Biochemistry, University of South Carolina, Columbia, SC 29205, USA

Abstract

C/EBP homologous protein (CHOP) is a transcription factor that is elevated in adipose tissue across many models of diabetes and metabolic stress. Although increased CHOP levels are associated with the terminal response to endoplasmic reticulum stress and apoptosis, there is no evidence for CHOP mediated apoptosis in the adipose tissue during diabetes. CHOP protein levels increase in parallel with protein succination, a fumarate derived cysteine modification, in the adipocyte during metabolic stress. We investigated the factors contributing to sustained CHOP proteins levels in the adipocyte, with an emphasis on the regulation of CHOP protein turnover by metabolite-driven modification of Keap1 cysteines. CHOP protein stability was investigated in conditions of nutrient stress due to high glucose or elevated fumarate (fumarase knockdown model); where cysteine succination is specifically elevated.

CHOP protein turnover is significantly reduced in models of elevated glucose and fumarate with a ~30% increase in CHOP stability ($p>0.01$), in part due to decreased CHOP phosphorylation. Sustained CHOP levels occur in parallel with elevated haem-oxygenase-1, a production of increased Nrf2 transcriptional activity and Keap1 modification. While Keap1 is directly succinated in the presence of excess fumarate derived from genetic knockdown of fumarase (fumarate levels are elevated >20-fold), it is the oxidative modification of Keap1 that predominates in adipocytes matured in high glucose (fumarate increases 4–5 fold). Elevated fumarate indirectly regulates CHOP stability through the induction of oxidative stress. The antioxidant N-acetylcysteine (NAC) reduces fumarate levels, protein succination and CHOP levels in adipocytes matured in high glucose. Elevated CHOP does not contribute elevated apoptosis in adipocytes, but plays a redox-dependent role in decreasing the adipocyte secretion of interleukin-13, an anti-inflammatory chemokine. NAC treatment restores adipocyte IL-13 secretion, confirming the redox-dependent regulation of a potent anti-inflammatory eotaxin.

*To whom correspondence should be addressed: Norma Frizzell, Department of Pharmacology, Physiology & Neuroscience, School of Medicine, University of South Carolina, 6439 Garners Ferry Road, Columbia, SC 29209, USA, Tel: (803) 216-3521; Fax: (803) 216-3538; norma.frizzell@uscmed.sc.edu.

This study demonstrates that physiological increases in the metabolite fumarate during high glucose exposure contributes to the presence of oxidative stress and sustained CHOP levels in the adipocyte during diabetes. The results reveal a novel metabolic link between mitochondrial metabolic stress and reduced anti-inflammatory adipocyte signaling as a consequence of reduced CHOP protein turnover.

Graphical Abstract

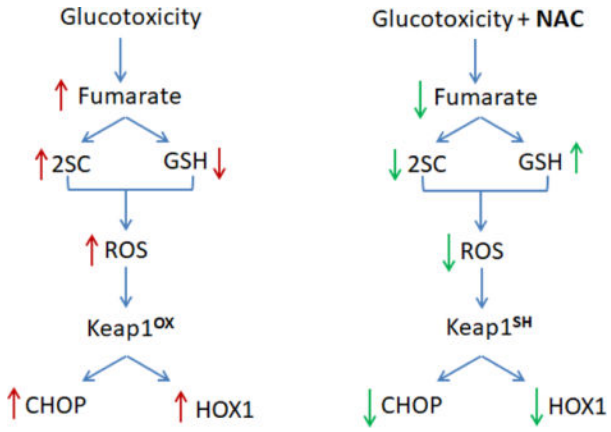

Keywords

Adipocytes; Metabolism; Adipose; Oxidative Stress; Glucotoxicity; Protein Modification; ER Stress

Introduction

The CCAAT enhancer binding protein (C/EBP) homologous protein (CHOP) is a basic leucine zipper transcription factor that can form heterodimers with the adipogenic transcription factors C/EBPα and C/EBPβ. CHOP binding of C/EBP isoforms suppresses adipogenic gene transcription due to the inability of the complex to interact with normal C/EBP binding sequences on the target gene (1, 2). The production of CHOP is upregulated in response to cellular stress including endoplasmic reticulum (ER) stress, oxidative stress, DNA damage, and hypoxia (3, 4, 5). The upregulation of CHOP as a consequence of ER stress has been documented in the adipose tissue of mouse models and human subjects (6, 7, 8, 9, 10, 11). We have observed that CHOP levels are strikingly elevated in adipocytes matured in high glucose versus normal glucose conditions, and this is associated with mitochondrial stress and reduced ER chaperone function during glucotoxicity (12, 13). The remarkably persistent levels of CHOP in parallel with mitochondrial stress appears to be independent of the activation of other markers of the unfolded protein response (UPR, 12), suggesting that CHOP levels are stabilized in the adipocyte during continued glucotoxicity.

Although elevated CHOP levels are typically associated with the induction of apoptosis during chronic ER stress (14), our recent data does not support a role for CHOP-mediated apoptosis in adipocytes (12). The accumulation of CHOP in the absence of apoptosis has

been described in the adipose tissue of obese insulin resistant patients (15), and insulin resistant mice (16). CHOP has alternative physiological roles in non-adipose cells including modulation of hepatocyte metabolic gene expression (17), adrenal steroid hormone synthesis (18) and chondrocyte survival (19).

CHOP is phosphorylated at Ser30 by several kinases; this inhibits transcriptional activity (20), and promotes the ubiquitination and proteasomal degradation of CHOP in macrophages (21). However, little is known about the mechanism regulating CHOP stability in the adipocyte during diabetes. Kelch-like ECH-associated protein 1 (Keap1) has been described as a negative regulator of CHOP stability in adipocytes, where Keap1 and cullin3 E3 ubiquitin ligase form a supercomplex with the COP9 signalosome (CSN) (22). CSN associated kinases, including CK2, further phosphorylate proteasome substrates to regulate protein stability (23). CHOP binds the CSN/cullin3 E3 ubiquitin ligase/Keap1 supercomplex, and this stimulates its degradation by the proteasome in adipocytes. The modification of stress-responsive Keap1 cysteines, and subsequent Keap1 degradation, may be a significant contributor to the sustained presence of CHOP during cellular stress. Keap1 contains 25 cysteine residues, 3 of these (Cys151, Cys273, Cys288) are confirmed sensors of oxidative stress that regulate the stabilization of nuclear factor (erythroid-derived 2)-like 2 (Nrf2) (24, 25, 26). Protein succination refers to the non-enzymatic Michael addition reaction between the Krebs cycle intermediate fumarate and available cysteine thiols to form the irreversible chemical modification S-(2-succino)cysteine (2SC) (27, 28). The 2SC modification (protein succination) has previously been detected on the regulatory Cys151 and Cys288 of Keap1 in *fumarase* (Fh1) deficient mouse embryonic fibroblasts (29). Fumarate ester treatment of neurons also results in the modification of Keap1 regulatory cysteines and the induction of the Nrf2 transcription program (30, 31). Nuclear accumulation of Nrf2 and upregulation of target antioxidant genes correlates directly with the succination of Keap1 (29, 30), confirming that fumarate is a physiologically relevant electrophilic activator of Nrf2 transcription.

The presence of excess fumarate results in a pronounced increase in protein succination in both adipocytes matured in high glucose, and in the adipose tissue of diabetic *db/db* and *ob/ob* mice (32, 33, 34). We have established that intracellular fumarate levels increase several fold in adipocytes matured in high glucose concentrations as a direct result of glucotoxicity driven mitochondrial stress (35, 13). Protein succination alters the structure and decreases the function of proteins such as adiponectin and protein disulfide isomerase in the adipocyte during glucotoxicity (33, 13). In the current study we investigated if fumarate is a novel metabolic regulator of CHOP stability in adipocytes during glucotoxicity. We hypothesized that direct succination of Keap1 may prevent CHOP degradation, thereby stabilizing CHOP protein levels. We demonstrate that the nature and extent of metabolic stress are model-dependent, and confirm that this influences CHOP protein stability in adipocytes. Alleviation of metabolic stress in adipocytes decreases CHOP stability and impacts IL-13 secretion in a CHOP-dependent manner.

Materials and Methods

Materials

Unless otherwise noted, all chemicals were purchased from Sigma Aldrich (St. Louis, MO). Insulin was purchased from Bio Ab Chem (Ladson, SC) for *in vitro* studies. Tween-20 and Criterion™ TGX™ Precast Gels were from Bio-Rad (Hercules, CA). Polyvinylidene fluoride (PVDF) was purchased from GE Healthcare (Fairfield, CT). L-glycine and sodium dodecyl sulfate (SDS) were purchased from Fisher Scientific (Waltham, MA).

Animal Models

Male *db/db* mice (BKS.Cg-Dock7^{m} +/+ Lepr^{db}/J, JAX 000642) and heterozygote control mice were purchased from Jackson Laboratories (Bar Harbor, ME). The mice were obtained at 5–6 weeks of age and were maintained with unrestricted access to food and water until 15 weeks of age. The mice were sacrificed at 15 weeks of age, at which time serum and adipose tissue depots were frozen for further analysis.

Protein Extraction from Adipose Tissue

Adipose tissue was homogenized in 0.5 – 5 mL radio immunoprecipitation assay (RIPA) buffer. A supernatant (lipid), infranatant and pellet were visible after centrifugation for 10 minutes at 5000 rpm. Acetone (9x volume) was then added to each extracted infranatant sample. The samples were vortexed, allowed to sit on ice for 10 minutes and then centrifuged at 2000 rpm for 10 minutes. The acetone was removed completely and the protein pellets were re-suspended in 0.3 – 1 mL of RIPA buffer. The protein concentration was determined using the Lowry method (36).

Cell Culture

3T3-L1 murine fibroblasts were purchased from American Type Culture Collection (Manassas, VA) and were differentiated and matured as previously described (12). Briefly, 5 mM glucose/0.3 nM insulin or 25 – 30 mM glucose/3 nM insulin was applied for ~8 days. These conditions were selected as we have observed that adipocytes cultured in normal glucose/insulin are a more appropriate control for the high glucose/insulin (diabetic) conditions normally used as control adipocyte conditions (12). The medium was changed every 48 hours, and the adipocytes were matured for 3, 5, 8 or 12 days. 10 μM MG132, 40 μM sulforaphane or 300 μM dimethyl fumarate (DMF) was added to the maturation medium 3 hours prior to harvest. In some cases cells were treated with 0, 2.5 or 5 mM N-acetylcysteine (NAC, prepared in DMEM, pH adjusted to 7.4). While we used tunicamycin to induce ER stress as a positive control for CHOP immunoblotting in some procedures, the data presented focuses on the induction and stability of CHOP in response to metabolic stress, rather than forced tunicamycin chemical stress. Cells cultured in 5 mM glucose were supplemented with 5 mM glucose daily and 5 hours prior to protein harvest to maintain glucose levels.

Lentiviral Vector Production & Transduction

The lentiviral vectors were prepared by the University of South Carolina Viral Vector Facility. Lentiviral vectors were generated using a transient transfection protocol, as described by Kantor *et al.* (37). TRC2 Fh1 shRNA, clone- TRCN0000246831 or SHC202 MISSION TRC2 pLKO.5-puro non-mammalian shRNA control plasmids (Sigma/Aldrich, St. Louis, MO) were used to generate the lentiviral vectors. The vectors also contained a puromycin resistance gene. 15 μg vector plasmid, 10 μg psPAX2 packaging plasmid (Addgene #12260, Cambridge, MA), 5 μg pMD2.G envelope plasmid (Addgene #12259, Cambridge, MA) and 2.5 μg pRSV-Rev plasmid (Addgene #12253, Cambridge, MA) were transfected into 293T cells. The filtered conditioned medium was collected and stored at −80°C until use. The Keap1-V5 overexpression plasmid was kindly provided by Dr. Anil Jaiswal, University of Maryland. The plasmid sequence was validated by PCR and cloned into a lentiviral vector containing green fluorescent protein (GFP) (pLenti-CMV-KEAP1-IRES-GFP). A vector containing the Keap1-V5 sequence in the opposite orientation was used as a control. The vector was produced as described above and the filtered conditioned medium was obtained following determination of the titer.

3T3-L1 fibroblasts were incubated overnight with 150 μL of filtered conditioned medium containing *Fh1* shRNA or scrambled control lentivirus. Successfully transduced fibroblasts were selected using 1 μg/mL puromycin. The selected fibroblasts were propagated until confluent, then differentiated to adipocytes and matured for 8 days in normal or high glucose as described above. 3T3-L1 fibroblasts or FHKD fibroblasts were differentiated as described above and transduced with the Keap1-V5 plasmid on maturation day 1. Over-expression of the Keap1 protein was monitored in adipocytes via green fluorescent protein through 5 or 8 days of maturation. Successful maturation in both glucose concentrations was confirmed by the accumulation of lipid droplets in the adipocyte by light microscopy (32, 12).

Measurement of Reactive Oxygen Species

FHKD or scrambled control adipocytes were matured in 5 mM or 30 mM glucose in serum free, phenol red free medium for 2.5 hours. 10 μM Amplex® UltraRed Reagent was added directly to the maturation medium. The fluorescence was recorded at 490_{ex} nm and 585_{em} nm every hour for 4 hours. Relative fluorescent units were normalized to total protein content per well following determination by the Lowry assay. FHKD or scrambled control adipocytes were matured for 2 days in 5 mM or 30 mM glucose medium. The cells were rinsed with sterile PBS and incubated for 45 minutes at 37°C with 500 μL serum free and phenol red free medium and 0.0065 μg/μL dichlorofluorescein (DCF). The DCF containing medium was removed and the cells were returned to maturation medium with serum free and phenol red free DMEM. Relative fluorescent units were measured at 485_{ex} nm and 535_{em} nm every 30 minutes for 4 hours and were normalized to the total protein content.

Cycloheximide Chase Assessment of CHOP Stability

3T3-L1 control or FHKD adipocytes were matured in 5 mM or 25 mM glucose for 8 days. Adipocytes (triplicate samples/group) were harvested at time point 0 hours and 3.5 μg/mL cycloheximide was added to four additional groups, which were then harvested every hour

for 4 hours. 10 μM MG132 was added to a separate group of adipocytes for 4 hours as a positive control to inhibit proteasomal CHOP degradation.

Glutathione and IL-13 Quantification

Adipocytes were matured for 8 days in the presence of 5 mM or 25 mM glucose with 0 or 5 mM NAC, or 100 μM DMF for 24 hours. Cellular protein was immediately precipitated using 5% salicyclic acid, sonicated and centrifuged at 14,000 rpm for 10 minutes. The supernatant was removed and total glutathione levels were quantified fluorimetrically according to the manufacturer's instructions (Arbor Assay Glutathione Fluorescent Detection Kit, Ann Arbor, MI). The media on 3T3-L1 adipocytes matured for 6 days was replaced with serum-free DMEM for 4 hours prior to collection of conditioned media. Secreted adipocyte IL-13 levels were quantified by ELISA according to the manufacturer's instructions (Interleukin-13 Mouse ELISA, Abcam, Cambridge, UK). Serum IL-13 and epididymal adipose tissue IL-13 levels from control and *db/db* diabetic mice were quantified using the same IL-13 ELISA. Adipose tissue IL-13 levels were normalized to the protein content of the sample.

Metabolite Quantification

The quantification of fumarate was performed by GC-MS at the David H. Murdock Research Institute (DHMRI, Kannapolis, NC). Metabolite extraction was performed in an adaptation of previous methods (38). Adipocyte lysates harvested in methanol from confluent 10 cm^2 petri dishes were washed three times with ice-cold PBS followed by the immediate addition of 20 volumes ice-cold chloroform:methanol (2:1). The samples were vortexed and allowed to stand on ice for 10 min with intermittent vortexing prior to addition of 0.2 volumes H_2O. The samples were sonicated and allowed to stand on ice for an additional 2 min, followed by centrifugation at 3,220 × g for 20 min. The aqueous supernatant was transferred into a clean tube and dried under air. The extraction was repeated an additional time by adding equal parts of methanol and deionized water, centrifuging, and transferring the aqueous layer into the respective tube to dry. The protein interface for each sample was removed for quantification of protein by the Lowry method.

Prior to derivatization the extracts were resuspended in ethyl acetate and transferred to GC-MS vials. The samples were dried with N_2, and an internal standard (100 μM succinate-$^{13}C_4$, Cambridge Isotope laboratories, Inc.) was added to each of the samples and fumarate standards. The samples and standards were derivatized with 200 μl of methylamine (20 mg/ml in pyridine, M.P. Biomedicals, Solon, OH) at 30°C for 90 min, followed by drying under N_2. This was followed by the addition of 120 μl of N-methyl-N-(trimethylsilyl) trifluoroacetamide (MSTFA, Sigma, St. Louis, MO) with 1% trimethylchlorosilane (TMCS, Sigma, St. Louis, MO); the mixture was incubated at 70°C for 60 min. The derivatized product was stored in a −20°C freezer for one hour prior to GC/MS analysis. An Agilent 7890A GC system, coupled to an Agilent 5975C electron ionization (EI) mass selective detector (MSD) was used to analyze the TMS-derivatized samples as described previously (38). Selected ion monitoring (SIM) was performed for fumarate and the peak areas obtained were normalized to the added internal standard. Absolute quantitation was

performed based on standard curves obtained from the normalized reference standards, and the final metabolite concentrations were normalized to the protein content of the cells.

Organelle Enrichment Fractionation

3T3-L1 adipocytes were matured for 8 days as described above. The cells were washed 3 times with ice cold PBS and once with homogenization buffer. The cells were scraped into 500 μL of homogenization buffer and lysed using a glass homogenizer before passing each lysate through a 25 gauge needle on ice. The samples were centrifuged at 500 × g for 10 minutes to generate the nuclear pellet, and the supernatant was removed and re-centrifuged at 10,000 × g for 20 minutes to produce the mitochondrial rich pellet and cytosolic supernatant.

Western Blotting

15–30 μg cell lysate protein or 30–100 μg mouse epididymal fat protein was subjected to SDS-PAGE on a BioRad Criterion system prior to immunoblotting as previously described (32). The membrane protein loading was visualized with Ponceau Red, followed by blocking in 5% bovine serum albumin (BSA) or 5% non-fat milk according to the antibody manufacturer's recommendations. The primary polyclonal antibody to actin (sc-1616) was from Santa Cruz Biotechnology Inc. (Dallas, TX). Polyclonal antibodies against fumarase (#4567), Keap1 (#4617), cleaved caspase 3 (#9664), and the monoclonal recognizing citrate synthase (#14309) were obtained from Cell Signaling (Danvers, MA). The anti-heme oxygenase1 antibody was from Enzo Life Sciences (ADI-SPA-896D) (Farmingdale, NY). The histone-H3 antibody (05928) was from Merck Millipore (Billerica, MA). The monoclonal antibody to CHOP (MA1–250) and the anti-V5-HRP linked (MA5–15253) antibody were from Pierce (Rockford, IL). The polyclonal anti-2SC antibody was prepared as described previously (32). Chemiluminescent substrate (Thermo Pierce, Rockford, IL) was utilized followed by detection on photographic film (Denville Scientific, Metuchen, NJ). Immunoblots were stripped (62.5 mM Tris, pH 6.8, 2% SDS and 0.7% (v/v) beta mercaptoethanol) for 20 minutes at 65°C prior to re-probing with new primary antibodies.

Protein Immunoprecipitation

Keap1 was immunoprecipitated from 400–800 μg of protein from control and FHKD adipocytes expressing the V5-Keap1 lentivirus using anti-V5 agarose affinity gel (Sigma Aldrich, St. Louis, MI), according to the manufacturer's instructions. The beads were washed 5 times with phosphate buffered saline and boiled with 2x Laemmli loading buffer for 5 minutes to remove the antibody-antigen complex.

Mass Spectrometry

Endogenous succination of Keap1 was identified following immunoprecipitation of the V5 tagged Keap1 protein over-expressed in FHKD adipocytes. The samples were resolved by SDS-PAGE, and the gel was stained with Coomassie Brilliant blue. After de-staining overnight, the protein was excised from the gel and washed in 20% methanol and 7% acetic acid solution to entirely remove the Coomassie blue stain. The samples were washed with 200 μL of 100 mM ammonium bicarbonate (pH 7.4) and dehydrated via acetonitrile and

vacuum centrifugation. The gel pieces were allowed to rehydrate in 10 mM DTT for 30 minutes at room temperature, followed by alkylation by 170 mM 4-vinylpyridine in methanol for 30 minutes. The pieces were washed twice with 100 mM ammonium bicarbonate and acetonitrile, completely dehydrated in the vacuum centrifuge, before rehydration in 50 mM ammonium bicarbonate buffer. Trypsin digestion was initiated with 2 pmol sequencing grade modified trypsin (Promega, Madison, WI) overnight at 37°C, as we have performed previously (31, 38). Peptides were then extracted from the gel using 4% formic acid and 20% acetonitrile solution and were concentrated to a total volume ~13 pL in the speed vacuum centrifuge prior to MS/MS analysis. Selected ion monitoring was performed to identify select pyridylethylated and succinated cysteine containing tryptic peptides. 1 μL of the digested samples were analyzed on a Dionex Ultimate 3000-LC system (Thermo Scientific, Rockford, IL) coupled to a Velos Pro Orbitrap mass spectrometer (Thermo Scientific, Rockford, IL). A 75-μm C18 stationary-phase LC column was used with a 60-min gradient from 2% acetonitrile in 0.1% formic acid solution (solvent A) to 70% solvent A and 30% solvent B (40% water in acetonitrile containing 0.1% formic acid). The Orbitrap was operated in data-dependent MS/MS analysis mode and excluded all ions below 200 counts. An inclusion list of up to 3 abundant isotopic masses +/− 2.5 amu was used to select the specific peptides for selected resonance monitoring and determination of the site of modification. To further identify specific succinated sites MRM was used to monitor select pyridylethylated and succinated tryptic peptide masses of interest (generated using Protein Calculator software) for CID (collision-induced dissociation)-MS/MS analysis. The data-dependent and CID-MS/MS data were analyzed using Proteome Discover 1.4 software with SEQUEST search engine against the *Mus musculus* proteome uniprot_database. The CID-MS/MS data was sequenced manually using Thermo Xcalibur 2.2 software to confirm the modified peptides. The variable modifications of methionine oxidation, proline hydroxylation, cysteine pyridylethylation (C^{PE}, 105.058 Da) or cysteine succination by fumarate (C^{2SC}, 116.011 Da) were considered in each data search.

Data Analysis

Image J software (National Institute of Health) was used to quantify band intensity by densitometry. All statistical analysis were preformed using Sigmaplot 11 software, using the student t-test or a one way ANOVA (n=3–6, *p< 0.05, or **p<0.01, ***p<0.001). Glutathione and IL-13 measurements were analyzed using a one way ANOVA (*p<0.05, **p< 0.01).

Results

CHOP protein levels are stabilized in the adipocyte

The unfolded protein response is activated early during adipogenesis (3, 39), followed by C/EBP homologous protein (CHOP) upregulation as the adipocytes mature. We have previously confirmed increased CHOP protein levels in adipocytes matured in normal (5 mM) and high glucose (25–30 mM) in the first 2 days of maturation (12). This transient increase in CHOP disappears by day 3 of maturation in normal glucose, while CHOP levels continue to increase in parallel with increasing protein succination for the duration of maturation in high glucose (Figure S1a, b)(12). Since adipocyte maturation and lipid

accumulation progress as expected in both glucose conditions, and other markers of the UPR resolve (12), we investigated why CHOP specifically remained elevated in the high glucose condition. To determine if glucotoxicity impairs CHOP turnover versus the continuous production of more CHOP, we performed a cycloheximide (CHX) chase experiment on adipocytes matured in 5 mM or 25 mM glucose for 8 days. CHOP stability was monitored over 4 hours, with the proteasomal inhibitor MG132 used as a positive control to allow CHOP accumulation (15). Sustained CHOP stability was observed in the absence of protein translation only in adipocytes matured in high glucose (Figure 1A), with a 29.5% increase in CHOP stability in adipocytes matured in high glucose versus normal glucose after 4 hours ($p<0.01$, Figure 1A). We have previously reported that lentiviral shRNA knockdown of fumarase expression results in a pronounced increase in both intracellular fumarate levels and protein succination in 3T3-L1 adipocytes matured in a normal glucose concentration (Figure S1c,d)(13). The CHX chase experiment was repeated in adipocytes transduced with a scrambled control or *fumarase* knockdown (FHKD) lentivirus, and cultured in 5 mM glucose to determine if protein succination has a direct role in preventing CHOP degradation, independent of elevated glucose concentrations. Similar to adipocytes matured in high glucose, FHKD adipocytes displayed a 28.5% increase in CHOP stability compared to the control cells after 4 hours ($n=3$, $p<0.01$, Figure 1B), confirming a role for increased fumarate in the regulation of CHOP turnover. Phosphorylation at Ser30 inhibits transcriptional activity and promotes proteasomal degradation of CHOP (20,21). Assessment of the phosphorylation status of CHOP Ser30 by immunoblotting demonstrated that CHOP phosphorylation did not increase in adipocytes matured in high glucose or FHKD conditions, despite the increased total CHOP levels when compared to respective controls (Figure 1C, D). These results confirm that CHOP is not only increased, but also stabilized during glucotoxicity and elevated fumarate, and further suggests that impaired phosphorylation of CHOP may prevent its degradation.

Modification of Keap1 cysteines enhances CHOP stability

Silencing of Keap1 expression increases the steady state level of CHOP in LiSa-2 adipocytes (22), emphasizing the importance of Keap1 as a regulator of CHOP turnover. We therefore sought to determine whether the modification of Keap1 regulatory cysteines contributes to CHOP stabilization. Since Keap1 is a low abundance cytosolic protein, both FHKD-scrambled control and FHKD adipocytes were transduced with a Keap1-V5 or a Keap1-V5-scrambled control lentivirus to obtain sufficient protein for analysis. A significant increase in protein succination in the FHKD adipocytes was confirmed with anti-2SC antibody (Figure 2A), concomitant with detection of both Keap1 and the V5 tag (Figure 2A). Immunoprecipitation of overexpressed Keap1-V5 demonstrated that Keap1 is succinated in the presence of abundant fumarate in FHKD adipocytes (Figure 2B). LC- MS/MS analysis following in-gel digestion identified the precise cysteine residue modified by fumarate. The top panel of Figure 2C displays the spectrum corresponding to the succinated peptide $^{288}C^{2SC}EILQADAR^{296}$ ($[M+2H]^{2+}$: 567.7625), containing the Keap1 regulatory Cys288. This result confirms the previous observation that Cys288 is a target of succination in *Fh1*$^{-/-}$ murine embryonic fibroblasts, where *Fh1* knockout also generates abundant fumarate (Adam 2011). The mass of the analogous control peptide containing the pyridylethyl (PE) cysteine

modification ($[M+2H]^{2+}$: 562.2803) was also detected (16.57 minutes, lower panel, Figure 2C).

The antioxidant sulforaphane and the fumarate ester dimethyl fumarate (DMF) are both known electrophilic modifiers of the redox sensitive cysteines of Keap1, resulting in the nuclear translocation of Nrf2 (30, 40, 41). Adipocytes were treated with 40 μM sulforaphane or 300 μM DMF for 3 hours, followed by detection of CHOP. The modification of Keap1 nucleophilic cysteines resulted in elevated CHOP protein levels (Figure 2D,E). Heme oxygenase (HOX1), an antioxidant protein upregulated in response to Nrf2 transcriptional activity (42), was also increased by both compounds (Figure 2D,E). This data establishes that the succination of Keap1 cysteines occurs in the presence of significant fumarate elevations, promoting the accumulation of CHOP.

Elevated fumarate induces oxidative stress to activate the Keap1/Nrf2 pathway

HOX1 protein levels were increased in adipocytes matured in 25 mM glucose; and in the epididymal adipose tissue of 15 wk old *db/db* mice compared to controls (Figure 3A, B), concomitant with increased Keap1 modification/Nrf2 activity. Increased HOX1 protein levels were also observed in the FHKD adipocytes (Figure 3C), which was expected given that elevated fumarate promotes Nrf2 transcriptional activity (29). Given that Keap1 is succinated in the FHKD adipocytes (Figure 2B,C), we next investigated if Keap1 is also succinated in adipocytes matured in high glucose, where fumarate levels are endogenously increased (Frizzell 2012). The successful transduction and overexpression of the Keap1-V5 lentivirus in adipocytes matured in 5 mM or 25 mM glucose was confirmed (Figure 3D). Surprisingly, immunoprecipitation of enriched Keap1 (black arrow, 73 kDa) failed to detect any succination of Keap1 in adipocytes matured in high glucose (Figure 3E) and was not evident by mass spectrometry.

Since the direct succination of Keap1 by fumarate in the high glucose environment could not be detected; we investigated if the oxidative modification of Keap1 thiols (25) might predominate in the high glucose environment. Analysis of reactive oxygen species (ROS) production by both Amplex Red® (hydrogen peroxide) and dichlorofluorescein (DCF) demonstrated a significant increase in ROS production in adipocytes matured in high glucose versus normal glucose (*$p<0.05$, Figure 3F,G). ROS levels were also increased in the FHKD adipocytes, and in adipocytes following brief treatment with DMF when cultured in normal glucose (*$p<0.05$, **$p<0.01$, Figure 3H), indicating that elevated fumarate is specifically capable of inducing oxidative stress in the adipocyte. The balance in the levels of fumarate and oxidants produced by the FHKD or high glucose adipocyte models likely determines whether Keap1 thiols are succinated or oxidized.

N-acetylcysteine reduces ROS and decreases CHOP stability, but differentially impacts fumarate levels in high glucose versus fumarase knockdown

The antioxidant N-acetylcysteine (NAC), pK_a ~9.5, reacts slowly with fumarate at physiological pH to form 2SC *in vitro* (27). NAC is a precursor for glutathione (GSH) synthesis (43, 44) and has some reactivity with fumarate in *Fh1* deficient cells (45). We investigated if NAC would impact fumarate levels and protein succination in adipocytes

matured in high glucose over 6–8 days. The quantification of intracellular fumarate levels following treatment of adipocytes with 0–5 mM NAC revealed that the 4-fold increase in intracellular fumarate concentrations were decreased ~2 and ~2.65 fold with 2.5 and 5 mM NAC, respectively (n=3, *p<0.05, ***p<0.001)(Figure 4A). Figure 4B demonstrates a concomitant decrease in total protein succination in adipocytes matured in high glucose in the presence of 2.5 or 5 mM NAC. This suggests that the NAC thiol moiety may react directly with endogenous fumarate to lower protein succination. The exogenous supply of NAC should also promote the synthesis of GSH. Total intracellular GSH was quantified in adipocytes matured in normal or high glucose in the presence of 5 mM NAC for 8 days, or 100 μM DMF for 24 hours (as a positive control to deplete GSH, 46). Total GSH levels were reduced by 36% in high glucose versus normal glucose (*p<0.05), whereas NAC protected against glucotoxicity induced oxidative stress by increasing GSH levels in high glucose (Figure 4C). ROS production in high glucose was also reduced in the presence of 1 mM NAC (Figure 4D,E). CHOP levels were markedly reduced in NAC-treated adipocytes; and this occurred in parallel with reduced HOX1 protein levels - a surrogate for decreased Nrf2 activity (Figure 4F). Therefore, in high glucose conditions NAC is capable of reducing fumarate and oxidant stress, decreasing Keap1 oxidative modification and reducing CHOP stability, as summarized in Figure 4G.

We next examined if NAC treatment would affect the FHKD adipocytes, where fumarate levels increase >20-fold versus ~4–5-fold in adipocytes matured in high glucose (Figure 5A vs. Figure 4A), FHKD adipocytes were cultured in normal glucose concentrations with 5 or 10 mM NAC for 8 days to determine if NAC affected fumarate levels and CHOP stability. Interestingly, treatment of FHKD adipocytes with NAC was not sufficient to reduce fumarate levels (Figure 5B), which contrasts with the NAC treatment of adipocytes matured in high glucose (Figure 4A). Fumarate levels increase to 5–10 mM in fumarase deficient cancers cells (47), therefore, the concentrations of NAC used (up to 5 mM) may not be sufficient to impact the more abundant increase in fumarate in this genetic model. NAC administration failed to reduce total protein succination levels, and unexpectedly the levels of succinated proteins increased in the presence of NAC in FHKD adipocytes (Figure 5C). This occurred in parallel with decreased levels of CHOP and HOX1 protein levels (Figure 5A). This suggested that the NAC mediated correction of oxidative stress contributed to lower CHOP levels, and that depletion of thiol oxidative stress by NAC might permit increased thiol reactivity of some thiols with fumarate, conversely increasing succination. To assess the oxidized thiol content we examined the levels of dimedone-stabilized cysteine sulfenic acids in mature FHKD adipocytes upon NAC treatment (48, 49). Immunoblotting to detect the dimedone adduct demonstrated a reduction in the profile of protein oxidation upon NAC treatment (Figure 5D). Overall, the data suggests that some competition may exist between fumarate and ROS for thiol reactivity within the FHKD adipocytes; a decrease in thiol oxidation due to NAC addition permitted the excess fumarate to irreversibly modify more cysteines by succination (Figure 5A,D).

2SC and CHOP accumulate in parallel in the absence of apoptosis

Figure 6 confirms the increased presence of CHOP in parallel with 2SC accumulation in adipocytes cultured in high glucose (Figure 6A), and the adipose tissue from *db/db* mice

(Figure 6B), as well as in FHKD adipocytes (Figure 6C). While CHOP is frequently associated with cleaved caspase 3 mediated apoptosis during severe ER stress (50), cleaved caspase 3 levels were unchanged in all models (Figure 6A,B,C). In addition, there were no morphological changes or loss of cell viability, protein content or change in nuclear content/structure, even in adipocytes matured in high glucose or FHKD adipocytes for as long as 12 days (Figure 6D, Figure S2a,b). These data suggest an alternative role for elevated CHOP in the mature adipocyte under conditions of metabolic stress.

CHOP accumulation is associated with impaired adipocyte IL-13 secretion

Biochemical fractions were prepared from adipocyte cell lysates to generate cytosolic, mitochondrial and nuclear-enriched fractions (Figure S3). CHOP accumulates in the nuclear fraction of adipocytes matured in 25 mM glucose versus 5 mM (Figure 7A), suggesting that CHOP has a continued role in transcription under diabetic conditions. Suzuki *et al.* have demonstrated that silencing CHOP expression improves the transcription and secretion of IL-13 in adipocytes, and in the adipose tissue of *CHOP* knockout mice fed a high fat diet (16). Therefore, we investigated if CHOP mediated IL-13 production is regulated by glucotoxicity-induced oxidative stress in the adipocyte as this may impact the inflammatory status of adipose tissue. IL-13 levels were quantified in conditioned medium collected from adipocytes cultured in 5 mM or 25 mM glucose +/− 5 mM NAC for 8 days (Figure 7B). While the levels of secreted IL-13 were reduced in adipocytes matured in high glucose by 70%, supplementation with NAC completely restored IL-13 secretion. Importantly, this data shows that oxidative stress underlies the nuclear CHOP mediated abolishment of IL-13 secretion in this model. Quantification of IL-13 levels in the adipose tissue and serum of *db/db* diabetic mice versus controls demonstrated that local adipocyte levels of IL-13 were reduced by ~60% in *db/db* mice (Figure 7D, p=0.004), in parallel with pronounced CHOP increases (Figure 7C), whereas serum levels of IL-13 levels were unchanged (Figure 7E). This suggests that the metabolic stress that drives increased CHOP has a significant impact on local IL-13 production, and these adipose tissue specific changes are not detected if only serum IL-13 is monitored.

Discussion

In this study we demonstrate that elevated fumarate and protein succination are associated with increased oxidative stress in the adipocyte, and that oxidative stress can promote the stable accumulation of CHOP and the suppression of anti-inflammatory IL-13 production. While CHOP is known to increase during the late stages of adipogenesis to restrict prolonged adipogenic signaling (3), we demonstrate for the first time that CHOP protein turnover is also markedly reduced during periods of nutrient-derived metabolic stress. We confirmed the expected increase in CHOP protein levels following adipocyte maturation in high glucose, and demonstrated that this is sustained only in high glucose, whereas CHOP induction is only transient in normal glucose (12). Since adipocytes matured in normal glucose differentiate and function normally, the transient induction of the UPR and CHOP are a regulated process; we and others have shown that UPR induction is a normal response to elevated insulin (10, 51, 52). In contrast, the stable accumulation of CHOP only appears to occur during continued metabolic stress in adipocytes and adipose tissue. Since we

observed sustained CHOP in parallel with increased protein succination (12), this suggested an association between mitochondrial stress, fumarate accumulation and CHOP stability. Proteasomal CHOP turnover was reduced during glucotoxicity, and during genetically induced fumarate accumulation. Despite this, we observed no increase in CHOP phosphorylation on Ser30, which is required for degradation, further suggesting that CHOP levels were increased and stable, or that degradation was impaired. The regulation of CHOP phosphorylation warrants further investigation in adipocytes, since AMP-activated protein kinase alpha has been shown to phosphorylate CHOP (21), and decreased in AMPK activity that has been described in obese, insulin resistant humans (53). Since CHOP ubiquitination and subsequent degradation is also regulated by the formation of a Keap1-dependent supercomplex in adipocytes, we hypothesized that succination of Keap1 in the presence of elevated fumarate (29, 30) may disturb CHOP interacting with the degradation supercomplex, thereby leading to CHOP accumulation. We confirmed that Keap1 is succinated on Cys288 in the intervening region (IVR) in *fumarase* knockdown (FHKD) adipocytes overexpressing Keap1. The modification of cysteines within the IVR domain is predicted to distort the tertiary structure of Keap1, impairing substrate ubiquitination and preventing protein:protein interactions in the Cullin-E3 ligase complex (54). Acute treatment with sulforaphane or dimethyl fumarate (DMF), both of which are electrophilic modifiers of Keap1 regulatory thiols, stabilized CHOP protein levels in the adipocyte.

In contrast to the FHKD adipocytes, we found no evidence of direct Keap1 succination by endogenously elevated fumarate in the adipocyte matured in high glucose (Figure 3C), despite observing activation of the Keap1/Nrf2/HOX1 signaling pathway in adipocytes *in vitro*, and the adipose tissue of *db/db* diabetic mice. This demonstrates that the dramatically increased levels of fumarate achieved using fumarase knockdown may lead to succination of targets that are not detected during endogenous fumarate elevations in adipocytes in high glucose. FHKD adipocytes allow the specific assessment of the contribution of fumarate to metabolic stress, independent of other glucose derived metabolites, but also represent a pronounced elevation in fumarate (20-fold increase versus ~4-fold increase in high glucose adipocytes versus control, Figures 5A & 6A). Genetic knockout and knockdown models are frequently employed to model tissue-specific metabolite stress (55, 56, 57), but these may not always exhibit the same concentrations observed in metabolic diseases such as obesity and diabetes, and may produce more pronounced effects on modified target proteins.

Considering that we could not detect direct Keap1 succination in the high glucose model, where fumarate is elevated in parallel with other sources of metabolic stress, we hypothesized that Keap1 thiol oxidation may prevail over succination, driving CHOP stability. Contrived mitochondrial derived ROS using antimycin A is associated with elevated CHOP in preadipocytes (4). ROS production is endogenously increased in adipocytes matured in high glucose (Figure 3F) (58, 59), as well as in FHKD adipocytes (Figure 3G), similar to the observed accumulation of ROS in *fumarase* deficient mouse kidney epithelial cells (45). The data demonstrates that specific increases in fumarate alone are sufficient to drive oxidative stress; and that mitochondrial derived metabolite stress and oxidant stress are inextricably linked. Reactive lipid aldehydes derived from superoxide and hydrogen peroxide irreversibly modify amino acid side chains; increasing protein carbonylation (60, 61). Total protein carbonylation positively correlates with growing

adiposity and increasing serum free fatty acid levels in obese adults (62), highlighting oxidative protein damage due to overnutrition. An acute study (6 days) of significant calorie excess in humans demonstrated that oxidative stress, rather than inflammation or ER stress, is the dominant, early contributor to deficient glucose uptake and decreased adipose tissue insulin sensitivity (63).

Considering the combined increase in mitochondrial fumarate and oxidative stress in adipocytes cultured in high glucose medium, we investigated if the antioxidant N-acetylcysteine (NAC) might have a beneficial action that would also impact the levels of protein succination. NAC treatment reduced the excess fumarate and lowered total protein succination in the adipocyte matured in high glucose in parallel with an anticipated decrease in ROS levels (Figure 4). While the reaction of NAC with fumarate is slow at physiological pH (27), it is significant that adipocytes matured in high glucose medium produce elevated citric acid cycle intermediates, as well as lactic acid, leading to an acidic microenvironment. Kulkarni *et al.* have recently demonstrated that protonated fumarate produced in acidic conditions may react more rapidly with thiols (64). The combination of fumarate hyperaccumulation and acidic pH both appear to contribute to the total levels of protein succination. The medium of adipocytes matured in high glucose conditions can reach pH 6.8 over the course of 48 hrs, and this may favor the reactivity of fumarate with NAC, decreasing the levels of total protein succination. In contrast, the FHKD adipocytes matured in normal glucose generate more fumarate, but the pH of the medium remains ~7.4. The absence of an acidic microenvironment may alter the reactivity of fumarate with NAC in the FHKD model (Figure 5 B,C). Indeed, we observed an increase in total protein succination in the presence of NAC. This suggested that by ameliorating oxidative stress, NAC reduced thiol oxidation and left more protein thiols available to react with the elevated fumarate concentration. This was supported by reduced sulfenylation of some proteins in the presence of NAC (Figure 5D). While there appears to be an anticorrelation between typically nucleophilic cysteines and fumarate reactive cysteines (64), it is conceivable that the modulation of nucleophilic thiols may structurally influence the reactivity of distal thiols, or that there is competition for some accessible thiols.

Despite differences in the factors that drive Nrf2 transcription and HOX1 protein increases in the high glucose and FHKD models, NAC treatment decreased HOX1 induction in both models, indicating suppression of Nrf2 transcriptional activity. The correction of oxidant damage by NAC in both models is sufficient to induce significant CHOP turnover by the intact Keap1/Cul3 complex, preventing Nrf2 displacement, as evidenced by parallel decreases in HOX1 expression.

CHOP induction is classically associated with apoptotic signaling cascades via transcriptional suppression of the pro-survival Bcl-2 family members (65), but recent work has elucidated additional roles independent of apoptosis (17, 18, 19). The accumulation of CHOP in adipocytes following proteasomal inhibition by MG132 has no effect on the protein levels of anti-apoptotic proteins Bcl-2 or Bax (15). Wild type and *CHOP* deficient mice fed a high fat diet display similar expression of Bcl-2 and CD95, and show no change in the ratio of TUNEL-positive cells to total nuclei, suggesting a limited role in apoptosis during obesity (16). Our observations in metabolically stressed adipocytes, and *db/db*

adipose tissue also confirm no evidence of apoptosis when CHOP is elevated. Instead, increases in caspase-1 mRNA and activation of the nucleotide-binding oligomerization domain-like receptor-3 (NLRP3) inflammasome lead to hypertrophic adipocyte death by pyroptosis, rather than CHOP-induced apoptosis, in the adipose tissue of *db/db, ob/ob*, and high fat diet fed mice (66).

Elevated CHOP in adipose tissue has been linked to inflammation mediated insulin resistance in mice fed a high fat diet, and *CHOP* knockout mice show a significant improvement in fasting blood glucose levels and insulin sensitivity after high fat diet feeding (7, 16). Interestingly, while the degree of macrophage infiltration does not change between wild type and *CHOP* knockout mice, adipose-specific CHOP deficiency promotes anti-inflammatory M2 macrophage polarization (7, 16). Further investigation on the functional role of CHOP in obese adipocytes demonstrated that upregulated CHOP could suppress IL-13 and IL-4 mRNA transcription, promoting M1 macrophage polarization in mice after 6 weeks of high fat diet feeding (16). Eosinophils are considered a predominant source of IL-4 and IL-13 in the adipose tissue microenvironment (67, 68), but the adipocytes themselves are an important source of IL-13 (69). *CHOP* knockout mice display upregulated transcription of eotaxins and increased eosinophil recruitment resulting in increased IL-4 levels, and the attenuation of inflammation in the adipose tissue microenvironment (16). Interestingly, IL-13 production was significantly higher in the adipocyte fraction of the CHOP knockout mouse adipose tissue, and adipocyte IL-13 contributed to beneficial M2 polarization. We confirmed that the nuclear accumulation of CHOP correlates with reduced adipocyte IL-13 secretion during maturation in high glucose versus normal glucose. Antioxidant treatment with NAC, which alleviates oxidative stress mediated CHOP stabilization (Figure 4), restores IL-13 secretion to the levels observed in adipocytes matured in normal glucose (Figure 7). The levels of IL-13 are also decreased in the *db/db* mouse versus controls, in parallel with elevated CHOP in the adipose tissue. The decrease in adipose tissue IL-13 was accompanied by no change in circulating serum IL-13 levels, further confirming that the local microenvironment has a large impact in determining the adipose tissue chemokine profile. The significance of the adipocyte as a regulator of adipose IL-13 production also explains why the rescue of obesity-related eosinophil deficiency did not substantially increase IL-13 expression (70), and further underscores the importance of understanding the metabolic stress that underlies adipocyte dysfunction and CHOP mediated transcriptional regulation. GATA3 and STAT5a transcription factors can bind the promotor region of the IL-13 gene, resulting in the upregulation of IL-13 mRNA transcription (71). Interestingly, GATA3 is expressed in white adipose tissue (72) and forms transcription factor complexes with C/EBPα and C/EBPβ to inhibit adipogenesis (73). It remains to be determined if stable nuclear CHOP interacts with anti-inflammatory transcription factor complexes containing GATA3 or STAT5a (74), thereby modulating the expression of chemokines affecting macrophage polarity, including IL-13.

In summary, we find that increased fumarate levels and protein succination are coupled to elevated oxidative stress; and that this leads to oxidative protein damage and impaired CHOP turnover in the adipocyte. Sustained CHOP protein levels in the nucleus correlates with decreased secretion of the anti-inflammatory cytokine IL-13. The improvement in IL-13 secretion following NAC treatment is a direct result of limiting oxidant-mediated

CHOP stabilization, emphasizing the importance of the intracellular oxidative environment and CHOP turnover for adipocyte functions that drive local macrophage polarity.

Supplementary Material

Refer to Web version on PubMed Central for supplementary material.

Acknowledgements

The authors would like to thank Dr. Boris Kantor (University of South Carolina Viral Vector Core, Columbia, SC) for generating and providing the *fumarase* shRNA and Keap1-V5 lentiviruses. The authors are grateful to Professor John Baynes (USC School of Medicine, Columbia, SC), for helpful discussion. This work was supported by grants from the American Diabetes Association (1-11-JF-13) and the National Institutes of Health (F31DK108559, R56DK105087, and R01NS92938).

List of Abbreviations

2SC	S-2(succino)cysteine
ATP	adenosine triphosphate
CCCP	carbonyl cyanide m-chlorophenyl hydrazone
C/EBP	CCAAT-enhancer binding protein
CHOP	C/EBP homologous protein
CHX	cycloheximide
CK2	casein kinase 2
CSN	COP9 signalosome
DAPI	4’,6-diamidino-2-phenylindole
DCF	dichlorofluorescein
DMF	dimethyl fumarate
DTPA	diethylenetriaminepentaacetic acid
Fh	fumarase
Fh1	fumarase hydratase gene
FHKD	fumarase knockdown
GSH	glutathione
HOX1	heme oxygenase 1
IL	interleukin
Keap1	Kelch-like associated protein 1
MEFs	mouse embryonic fibroblasts

m/z	mass/charge ratio
NAC	n-acetylcysteine
NADH	nicotinamide adenine dinucleotide
NRF2	nuclear factor (erythroid-derived 2)-like 2
PE	pyridylethylation
PPARγ	peroxisome proliferator-activated receptor gamma
RFU	relative fluorescence units
RIPA	radioimmunoprecipitation assay buffer
ROS	reactive oxygen species
shRNA	short hairpin ribonucleic acid

References

1. Ubeda M, Wang XZ, Zinszner H, Wu I, Habener JF, Ron D. Stress-induced binding of the transcriptional factor CHOP to a novel DNA control element. Molecular and Cellular Biology. 1996;16(4):1479–1489. [PubMed: 8657121]
2. Batchvarova N, Wang XZ, Ron D. Inhibition of adipogenesis by the stress-induced protein CHOP (Gadd153). EMBO Journal. 1995;14(19):4654–4661. [PubMed: 7588595]
3. Han J, Murthy R, Wood B, Song B, Wang S, Sun B, Malhi H, Kaufman RJ. ER stress signalling through eIF2 and CHOP, but not IRE1, attenuates adipogenesis in mice. Diabetologia. 2013;56(): 911–924. [PubMed: 23314846]
4. Carrière A, Carmona MC, Fernandez Y, Rigoulet M, Wenger RH, Pénicaud L, Casteilla L. Mitochondrial reactive oxygen species control the transcription factor CHOP-10/GADD153 and adipocyte differentiation: a mechanism for hypoxia-dependent effect. Journal of Biological Chemisty;279(39) 40462–40469.
5. Luethy JD, Holbrook NJ. Activation of the gadd153 promoter by genotoxic agents: a rapid and specific response to DNA damage. Cancer Research. 1992;52(1):5–10. [PubMed: 1727386]
6. Boden G, Duan X, Homko C, Molina EJ, Song W, Perez O, Cheung P, Merali S. Increase in endoplasmic reticulum stress-related proteins and genes in adipose tissue of obese, insulin-resistant individuals. Diabetes. 2008;57(9):2438–2444. [PubMed: 18567819]
7. Maris M, Overbergh L, Gysemans C, Waget A, Cardozo AK, Verdrengh E, Cunha JP, Gotoh T, Cnop M, Eizirik DL, Burcelin R, Mathieu C. Deletion of C/EBP homologous protein (Chop) in C57Bl/6 mice dissociates obesity from insulin resistance. Diabetologia. 2012;55(4): 1167–1178. [PubMed: 22237685]
8. Kawasaki N, Asada R, Saito A, Kanemoto S, Imaizumi K. Obesity-induced endoplasmic reticulum stress causes chronic inflammation in adipose tissue. Science Reports. 2012;2:799.
9. Liong S, Lappas M. Endoplasmic reticulum stress is increased in adipose tissue of women with gestational diabetes. PLoS One. 2015;10:e0122633 [PubMed: 25849717]
10. Özcan U, Cao Q, Yilmaz E, Lee AH, Iwakoshi NN, Ozdelen E, Tuncman G, Görgün C, Glimcher LH, Hotamisligil GS. Endoplasmic reticulum stress links obesity, insulin action, and type 2 diabetes. Science. 2004;306(5695):457–461. [PubMed: 15486293]
11. Sharma NK, Das SK, Mondal AK, Hackney OG, Chu WS, Kern PA, Rasouli N, Spencer HJ, Yao-Borengasser A, Elbein SC. Endoplasmic reticulum stress markers are associated with obesity in nondiabetic subjects. Journal of Clinical Endocrinology and Metabolism. 2008;93(11):4532–4541. [PubMed: 18728164]

12. Tanis RM, Piroli GG, Day SD, Frizzell N. The effect of glucose concentration and sodium phenylbutyrate treatment on mitochondrial bioenergetics and ER stress in 3T3-L1 adipocytes. Biochimica et Biophysica Acta. 2015;1853(1): 213–221. [PubMed: 25448036]

13. Manuel AM, Walla MD, Faccenda A, Martin SL, Tanis RM, Piroli GG, Adam J, Kantor B, Mutus B, Townsend DM, Frizzell N. Succination of Protein Disulfide Isomerase Links Mitochondrial Stress and Endoplasmic Reticulum Stress in the Adipocyte During Diabetes. Antioxidants and Redox Signaling. 2017; 27(16):1281–1296 [PubMed: 28376661]

14. Song B, Scheuner D, Ron D, Pennathur S, Kaufman RJ. Chop deletion reduces oxidative stress, improves beta cell function, and promotes cell survival in multiple mouse models of diabetes. J Clin Invest. 2008 10;118(10):3378–89. [PubMed: 18776938]

15. Díaz-Ruiz A, Guzmán-Ruiz R, Moreno NR, García-Rios A, Delgado-Casado N, Membrives A, Túnez I, El Bekay R, Fernández-Real JM, Tovar S, Diéguez C, Tinahones FJ, Vázquez-Martínez R, López-Miranda J, Malagón MM. Proteasome Dysfunction Associated to Oxidative Stress and Proteotoxicity in Adipocytes Compromises Insulin Sensitivity in Human Obesity. Antioxidants and Redox Signaling. 2015;23(7): 597–612. [PubMed: 25714483]

16. Suzuki T, Gao J, Ishigaki Y, Kondo K, Sawada S, Izumi T, Uno K, Kaneko K, Tsukita S, Takahashi K, Asao A, Ishii N, Imai J, Yamada T, Oyadomari S, Katagiri H. ER Stress Protein CHOP Mediates Insulin Resistance by Modulating Adipose Tissue Macrophage Polarity. Cell Reports. 2017;18(8): 2045–2057. [PubMed: 28228268]

17. Chikka MR, McCabe DD, Tyra HM, Rutkowski DT. C/EBP homologous protein (CHOP) contributes to suppression of metabolic genes during endoplasmic reticulum stress in the liver. Journal of Biological Chemistry. 2013;288(6): 4405–4415. [PubMed: 23281479]

18. Prasad M, Walker AN, Kaur J, Thomas JL, Powell SA, Pandey AV, Whittal RM, Burak WE, Petruzzelli G, Bose HS. Endoplasmic Reticulum Stress Enhances Mitochondrial Metabolic Activity in Mammalian Adrenals and Gonads. Molecular and Cellular Biology. 2016;36(24): 3058–3074. [PubMed: 27697863]

19. Wang C, Tan Z, Niu B, Tsang KY, Tai A, Chan WCW, Lo RLK, Leung KKH, Dung NWF, Itoh N, Zhang MQ, Chan D, Cheah KSE. Inhibiting the integrated stress response pathway prevents aberrant chondrocyte differentiation thereby alleviating chondrodysplasia. Elife. 2018;19;7 pii: e37673.

20. Ubeda M, Habener JF. CHOP transcription factor phosphorylation by casein kinase 2 inhibits transcriptional activation. Journal of Biological Chemistry. 2003;278(42):40514–40520. [PubMed: 12876286]

21. Dai X, Ding Y, Liu Z, Zhang W, Zou MH. Phosphorylation of CHOP (C/EBP Homologous Protein) by the AMP-Activated Protein Kinase Alpha 1 in Macrophages Promotes CHOP Degradation and Reduces Injury-Induced Neointimal Disruption In Vivo. Circulation Research. 2016;119(10): 1089–1100. [PubMed: 27650555]

22. Huang X, Ordemann J, Muller JM, Dubiel W. The COP9 signalosome, cullin 3 and Keap1 supercomplex regulates CHOP stability and adipogenesis. Biology Open. 2012;1(8):705–710. [PubMed: 23213463]

23. Hannss R, Dubiel W. COP9 signalosome function in the DDR. FEBS Letters. 2011;585(18): 2845–2852. [PubMed: 21510940]

24. McMahon M, Lamont DJ, Beattie KA, Hayes JD Keap1 perceives stress via three sensors for the endogenous signaling molecules nitricoxide, zinc, and alkenals. Proceedings of the National Academy of Sciences of the United States of America. 2010;107(44): 18838–18843. [PubMed: 20956331]

25. Kobayashi A, Kang MI, Watai Y, Tong KI, Shibata T, Uchida K, Yamamoto M. Oxidative and electrophilic stresses activate Nrf2 through inhibition of ubiquitination activity of Keap1. Molecular and Cellular Biology. 2006;26(1): 221–229. [PubMed: 16354693]

26. Levonen AL, Landar A, Ramachandran A, Ceaser EK, Dickinson DA, Zanoni G, Morrow JD, Darley-Usmar VM. Cellular mechanisms of redox cell signalling: role of cysteine modification in controlling antioxidant defenses in response to electrophilic lipid oxidation products. Biochemical Journal. 2004; 378(Pt2):373–382. [PubMed: 14616092]

27. Alderson NL, Wang Y, Blatnik M, Frizzell N, Walla MD, Lyons TJ, Alt N, Carson JA, Nagai R, Thorpe SR, Baynes JW. S-(2-Succinyl)cysteine: a novel chemical modification of tissue proteins

by a Krebs cycle intermediate. Archives of Biochemistry and Biophysics. 2006;450(1): 1–8. [PubMed: 16624247]

28. Merkley ED, Metz TO, Smith RD, Baynes JW, Frizzell N. The succinated proteome. Mass Spectrom Rev. 2014 Mar-Apr;33(2):98–109. [PubMed: 24115015]
29. Adam J, Hatipoglu E, O'Flaherty L, Ternette N, Sahgal N, Lockstone H, Baban D, Nye E, Stamp GW, Wolhuter K, Stevens M, Fischer R, Carmeliet P, Maxwell PH, Pugh CW, Frizzell N, Soga T, Kessler BM, El-Bahrawy M, Ratcliffe PJ, Pollard PJ. Renal cyst formation in Fh1-deficient mice is independent of the Hif/Phd pathway: roles for fumarate in KEAP1 succination and Nrf2 signaling. Cancer Cell. 2011;20(4):524–537. [PubMed: 22014577]
30. Linker RA, Lee DH, Ryan S, van Dam AM, Conrad R, Bista P, Zeng W, Hronowsky X, Buko A, Chollate S, Ellrichmann G, Bruck W, Dawson K, Goelz S, Wiese S, Scannevin RH, Lukashev M, Gold R. Fumaric acid esters exert neuroprotective effects in neuroinflammation via activation of the Nrf2 antioxidant pathway. Brain. 2011;134(Pt3): 678–692. [PubMed: 21354971]
31. Piroli GG, Manuel AM, Patel T, Walla MD, Shi L, Lanci SA, Wang J, Galloway A, Ortinski PI, Smith DS, Frizzell N. Identification of Novel Protein Targets of Dimethyl Fumarate Modification in Neurons and Astrocytes Reveals Actions Independent of Nrf2 Stabilization. Mol Cell Proteomics. 2019;18(3):504–519. [PubMed: 30587509]
32. Nagai R, Brock JW, Blatnik M, Baatz JE, Bethard J, Walla MD, Thorpe SR, Baynes JW, Frizzell N. Succination of Protein Thiols During Adipocyte Maturation: A Biomarker of Mitochondrial Stress. Journal of Biological Chemistry. 2007;282(47): 34219–34228. [PubMed: 17726021]
33. Frizzell N, Rajesh M, Jepson M, Nagai R, Carson JA, Thorpe SR, and Baynes JW. Succination of Thiol Groups in Adipose Tissue Proteins in Diabetes Succination Inhibits Polymerization and Secretion of Adiponectin. Journal of Biological Chemistry. 2009;284(38): 25772–25781. [PubMed: 19592500]
34. Thomas SA, Storey KB, Baynes JW, Frizzell N. Tissue distribution of S-(2-succino)cysteine (2SC), a biomarker of mitochondrial stress in obesity and diabetes. Obesity (Silver Spring). 2012;20(2): 263–269. [PubMed: 22134201]
35. Frizzell N, Thomas SA, Carson JA, Baynes JW. Mitochondrial stress causes increased succination of proteins in adipocytes in response to glucotoxicity. Biochemical Journal. 2012;44(2):247–254.
36. Lowry OH, Rosebrough NJ, Farr AL, and Randall RJ Protein measurement with the Folin phenol reagent. Journal of Biological Chemistry. 1951; 193, 265–275 [PubMed: 14907713]
37. Kantor B, Bayer M, Ma H, Samulski J, Li C, McCown T, Kafri T. Notable reduction in illegitimate integration mediated by a PPT-deleted, nonintegrating lentiviral vector. Molecular Therapy. 2011;19(3): 547–556. [PubMed: 21157436]
38. Piroli GG, Manuel AM, Clapper AC, Walla MD, Baatz JE, Palmiter RD, Quintana A, Frizzell N. Succination is increased on select proteins in the brainstem of the Ndufs4 knockout mouse, a model of Leigh syndrome. Molecular and Cellular Proteomics. 2016;15(2): 445–461. [PubMed: 26450614]
39. Basseri S, Lhoták Š, Sharma A, Austin RC. The chemical chaperone 4-phenylbutyrate inhibits adipogenesis by modulating the unfolded protein response. Journal of Lipid Research. 2009;50(12): 2486–2501. [PubMed: 19461119]
40. Hong F, Freeman ML, Liebler DC. Identification of sensor cysteines in human Keap1 modified by the cancer chemopreventive agent sulforaphane. Chemical Research in Toxicology. 2005;18(12): 1917–1926. [PubMed: 16359182]
41. Hu C, Eggler AL, Mesecar AD, van Breemen RB. Modification of keap1 cysteine residues by sulforaphane. Chemical Research in Toxicology. 2011;24(4): 515–521. [PubMed: 21391649]
42. Alam J, Stewart D, Touchard C, Boinapally S, Choi AMK and Cook JL. Nrf2, a Cap'n'Collar Transcription Factor, Regulates Induction of the Heme Oxygenase-1 Gene. Journal of Biological Chemistry. 1999;274(37): 26071–26078. [PubMed: 10473555]
43. Medved I, Brown MJ, Bjorksten AR, Murphy KT, Petersen AC, Sostaric S, Gong X, McKenna MJ. N-acetylcysteine enhances muscle cysteine and glutathione availability and attenuates fatigue during prolonged exercise in endurance-trained individuals. Journal of Applied Physiology. 2004;97(4): 14771485.

44. Phelps DT, Deneke SM, Daley DL, Fanburg BL. Elevation of glutathione levels in bovine pulmonary artery endothelial cells by N-acetylcysteine. American Journal of Respiratory Cell and Molecular Biology. 1992;7(3): 293–299. [PubMed: 1520492]
45. Zheng L, Cardaci S, Jerby L, MacKenzie ED, Sciacovelli M, Johnson TI, Gaude E, King A, Leach JD, Edrada-Ebel R, Hedley A, Morrice NA, Kalna G, Blyth K, Ruppin E, Frezza C, Gottlieb E. Fumarate induces redox-dependent senescence by modifying glutathione metabolism. Nature Communications. 2015;6:6001.
46. Manuel AM, Frizzell N. Adipocyte protein modification by Krebs cycle intermediates and fumarate ester-derived succination. Amino Acids. 2013;45(5): 1243–1247. [PubMed: 23892396]
47. Ternette N, Yang M, Laroyia M, Kitagawa M, O'Flaherty L, Wolhulter K, Igarashi K, Saito K, Kato K, Fischer R. Inhibition of Mitochondrial Aconitase by Succination in Fumarate Hydratase Deficiency. Cell Reports. 2013;3(3): 689–700. [PubMed: 23499446]
48. Martínez-Acedo P, Gupta V, Carroll KS. Proteomic analysis of peptides tagged with dimedone and related probes. Journal of Mass Spectrometry. 2014;49(4): 257–265. [PubMed: 24719340]
49. Seo YH, Carroll KS. Quantification of protein sulfenic acid modifications using isotope-coded dimedone and iododimedone. Angewandte Chemie International ed. English 2011;50(6): 1342–1345.
50. Li Y, Guo Y, Tang J, Jiang J, Chen Z. New insights into the roles of CHOP-induced apoptosis in ER stress. Acta Biochimica et Biophysica Sin. 2014;46(2): 629–640.
51. Boden G, Cheung P, Salehi S, Homko C, Loveland-Jones C, Jayarajan S, Stein TP, Williams KJ, Liu ML, Barrero CA, Merali S. Insulin regulates the unfolded protein response in human adipose tissue. Diabetes. 2014 3;63(3):912–22. [PubMed: 24130338]
52. Minard AY, Wong MK, Chaudhuri R, Tan SX, Humphrey SJ, Parker BL, Yang JY, Laybutt DR, Cooney GJ, Coster AC, Stöckli J, James DE. Hyperactivation of the Insulin Signaling Pathway Improves Intracellular Proteostasis by Coordinately Up-regulating the Proteostatic Machinery in Adipocytes. J Biol Chem. 2016;291(49):25629–25640. [PubMed: 27738101]
53. Gauthier M-S, O'Brien EL, Bigornia S, Mott M, Cacicedo JM, Xu XJ, Gokce N, Apovian C, Ruderman N 2011 Decreased AMP-activated protein kinase activity is associated with increased inflammation in visceral adipose tissue and with whole-body insulin resistance in morbidly obese humans. Biochem. Biophys. Res. Commun 404: 382–387 [PubMed: 21130749]
54. Canning P, Sorrell FJ, Bullock AN. Structural basis of Keap1 interactions with Nrf2. Free Radical Biology and Medicine. 2015;88(Pt B): 101–107. [PubMed: 26057936]
55. Nishida Y, Rardin MJ, Carrico C, He W, Sahu AK, Gut P, Najjar R, Fitch M, Hellerstein M, Gibson BW, Verdin E. SIRT5 Regulates both Cytosolic and Mitochondrial Protein Malonylation with Glycolysis as a Major Target. Molecular Cell. 2015;59(2): 321–332. [PubMed: 26073543]
56. Park J, Chen Y, Tishkoff DX, Peng C, Tan M, Dai L, Xie Z, Zhang Y, Zwaans BM, Skinner ME, Lombard DB, Zhao Y. SIRT5-mediated lysine desuccinylation impacts diverse metabolic pathways. Molecular Cell. 2013;50(6): 919–930. [PubMed: 23806337]
57. Wagner GR, Bhatt DP, O'Connell TM, Thompson JW, Dubois LG, Backos DS, Yang H, Mitchell GA, Ilkayeva OR, Stevens RD, Grimsrud PA, Hirschey MD. A Class of Reactive Acyl-CoA Species Reveals the Non-enzymatic Origins of Protein Acylation. Cell Metabolism. 2017;25(4): 823–837. [PubMed: 28380375]
58. Han CY. Roles of Reactive Oxygen Species on Insulin Resistance in Adipose Tissue. Diabetes and Metabolism Journal. 2016;40(4): 272–279. [PubMed: 27352152]
59. Lin Y, Berg AH, Iyengar P, Lam TK, Giacca A, Combs TP, Rajala MW, Du X, Rollman B, Li W, Hawkins M, Barzilai N, Rhodes CJ, Fantus IG, Brownlee M, Scherer PE. The hyperglycemia-induced inflammatory response in adipocytes: the role of reactive oxygen species. Journal of Biological Chemistry. 2005;280(6): 4617–4626. [PubMed: 15536073]
60. Circu ML, Aw TY. Reactive oxygen species, cellular redox systems, and apoptosis. Free Radical Biology and Medicine. 2010;48(6): 749–762. [PubMed: 20045723]
61. Curtis JM, Hahn WS, Stone MD, Inda JJ, Droullard DJ, Kuzmicic JP, Donoghue MA, Long EK, Armien AG, Lavandero S, Arriaga E, Griffin TJ, Bernlohr DA. Protein carbonylation and adipocyte mitochondrial function. Journal of Biological Chemistry. 2012;287(39): 32967–32980. [PubMed: 22822087]

62. Frohnert BI, Sinaiko AR, Serrot FJ, Foncea RE, Moran A, Ikramuddin S, Choudry U, Bernlohr DA. Increased adipose protein carbonylation in human obesity. Obesity (Silver Spring). 2011;19(9): 1735–1741. [PubMed: 21593812]

63. Boden G, Homko C, Barrero CA, Stein TP, Chen X, Cheung P, Fecchio C, Koller S, Merali S. Excessive caloric intake acutely causes oxidative stress, GLUT4 carbonylation, and insulin resistance in healthy men. Science Translational Medicine. 2015;7(304): 304re7.

64. Kulkarni RA, Bak DW, Wei D, Bergholtz SE, Briney CA, Shrimp JH, Alpsoy A, Thorpe AL, Bavari AE, Crooks DR, Levy M, Florens L, Washburn MP, Frizzell N, Dykhuizen EC, Weerapana E, Linehan WM, Meier JL. A chemoproteomic portrait of the oncometabolite fumarate. Nature Chemical Biology. 2019;15(4):391–400. [PubMed: 30718813]

65. Cullough KM, Martindale JL, Klotz LO, Aw TY, Holbrook NJ. Gadd153 sensitizes cells to endoplasmic reticulum stress by down-regulating Bcl2 and perturbing the cellular redox state, Mol Cell Biol, 2001; 21(246–259)

66. Giordano A, Murano I, Mondini E, Perugini J, Smorlesi A, Severi I, Barazzoni R, Scherer PE, Cinti S. Obese adipocytes show ultrastructural features of stressed cells and die of pyroptosis. Journal of Lipid Research. 2013;54(9): 2423–2436. [PubMed: 23836106]

67. Lumeng CN, Bodzin JL, Saltiel AR. Obesity induces a phenotypic switch in adipose tissue macrophage polarization. Journal of Clinical Investigation, 2007;117(175–184) [PubMed: 17200717]

68. Bolus WR, Kennedy AJ, Hasty AH. Obesity-induced reduction of adipose eosinophils is reversed with low-calorie dietary intervention. Physiol Rep. 2018;6(22):e13919. [PubMed: 30488596]

69. Kang K, Reilly SM, Karabacak V, Gangl MR, Fitzgerald K, Hatano B, Lee CH. Adipocyte-derived Th2 cytokines and myeloid PPARdelta regulate macrophage polarization and insulin sensitivity. Cell Metabolism. 2008;7(6):485–95 [PubMed: 18522830]

70. Bolus WR, Peterson KR, Hubler MJ, Kennedy AJ, Gruen ML, Hasty AH. Elevating adipose eosinophils in obese mice to physiologically normal levels does not rescue metabolic impairments. Molecular Metabolism. 2018;8:86–95. [PubMed: 29306658]

71. Wei G, Abraham BJ, Yagi R, Jothi R, Cui K, Sharma S, Narlikar L, Northrup DL, Tang Q, Paul WE, Zhu J, Zhao K. Genome-wide analyses of transcription factor GATA3-mediated gene regulation in distinct T cell types. Immunity. 2011;35(2): 299–311. [PubMed: 21867929]

72. Tong Q, Dalgin G, Xu H, Ting CN, Leiden JM, Hotamisligil GS. Function of GATA transcription factors in preadipocyte-adipocyte transition. Science. 2000;290(5489):134–138. [PubMed: 11021798]

73. Tong Q, Tsai J, Tan G, Dalgin G, Hotamisligil GS. Interaction between GATA and the C/EBP family of transcription factors is critical in GATA-mediated suppression of adipocyte differentiation. Molecular and Cellular Biology. 2005;25(2): 706–715. [PubMed: 15632071]

74. Zhu J T helper 2 (Th2) cell differentiation, type 2 innate lymphoid cell (ILC2) development and regulation of interleukin-4 (IL-4) and IL-13 production. Cytokine. 2015;75(1): 14–24. [PubMed: 26044597]

Highlights

- CHOP protein turnover and phosphorylation is reduced in the white adipocyte
- Increased fumarate contributes to oxidative stress in models of metabolic stress
- Keap1 thiols are modified by fumarate or oxidants, preventing CHOP turnover
- Elevated CHOP leads to reduced adipocyte IL-13 *in vitro* and in db/db adipose tissue
- N-acetylcysteine reduces CHOP levels and improves IL-13 secretion

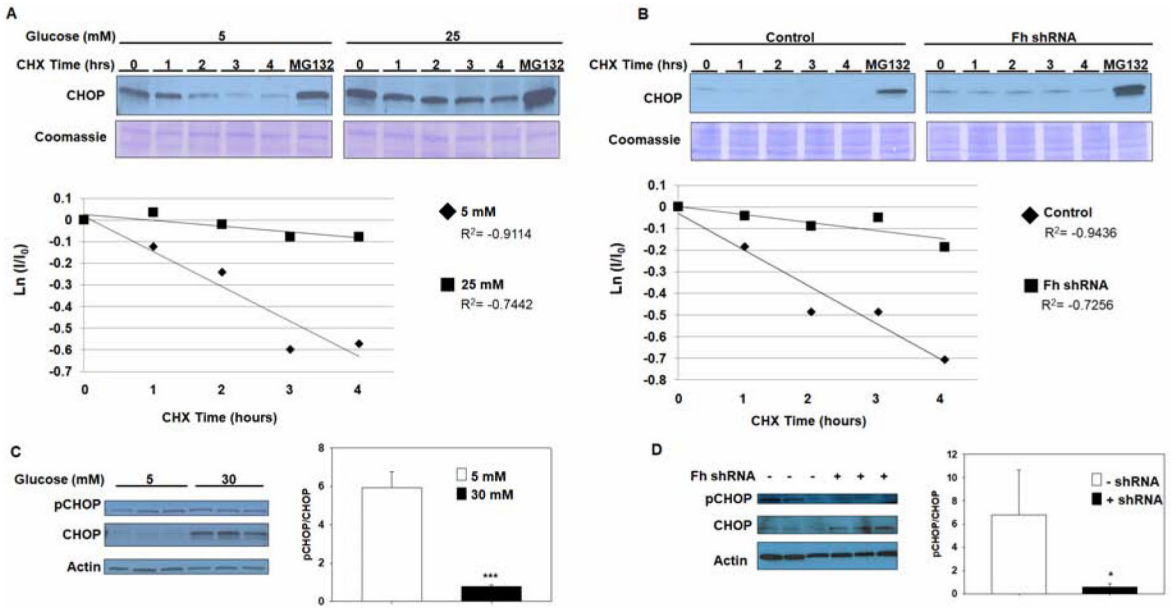

Figure 1: CHOP turnover decreases during metabolic stress in the adipocyte

(A) 3T3-L1 adipocytes were matured in 5 mM or 25 mM glucose or (B) transduced with either scrambled control or *fumarase* (Fh) knockdown shRNA (FHKD), and matured in 5 mM glucose for 8 days. Protein synthesis was inhibited with 3.5 μg/mL cycloheximide (CHX) and the adipocytes in each group were harvested at the indicated times (hrs) after addition of CHX. CHOP protein levels over time are shown by immunoblotting with anti-CHOP antibody and Coomassie blue staining represents equal protein loading. The graphs display the natural logarithm of the relative levels of CHOP as a function of CHX chase time. n=3/group for all treatments, $p<0.01$ at 4 hours. (C) The levels of phosphorylated CHOP (pSer30) were compared to total levels of CHOP in adipocytes during normal and high glucose exposure, or (D) upon shRNA knockdown of Fh. pCHOP levels were normalized to total CHOP protein levels. Despite the pronounced increase in CHOP levels, the level of CHOP phosphorylation is not increased when glucose or fumarate are elevated. Representative experiments are shown with n=3 per group for immunoblots.

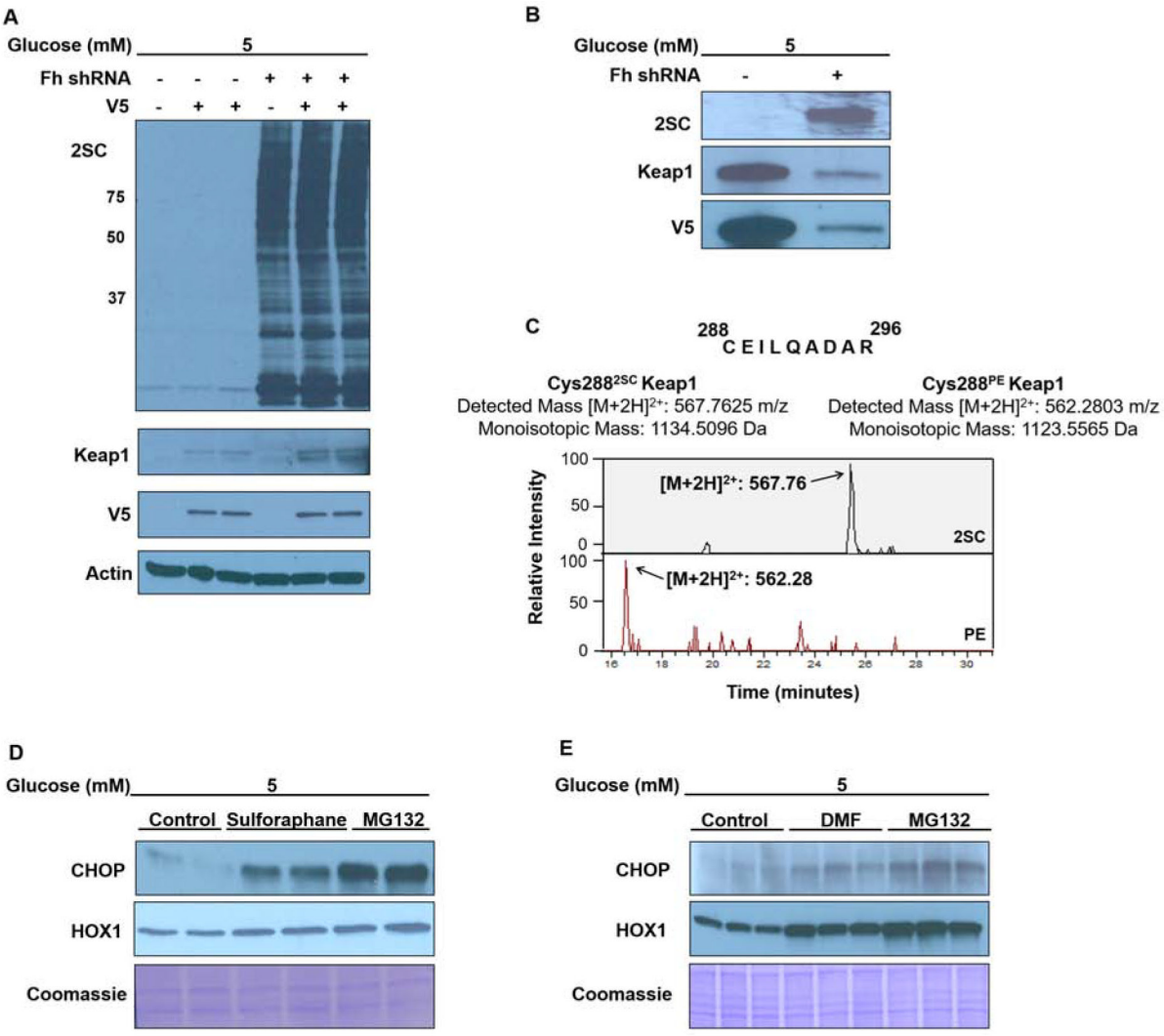

Figure 2: Keap1 cysteine modification increases CHOP stability and HOX1 protein levels

(A) Control and *fumarase* knockdown (FHKD) adipocytes were transduced with the Keap1-V5 tagged or empty control lentivirus. Immunoblotting with anti-2SC confirms increased protein succination in adipocytes following shRNA knockdown of Fh (FHKD) versus the scrambled control. The overexpression of Keap1 protein was confirmed Keap1 and V5 antibodies. (B) Keap1 was immunoprecipitated with anti-V5 agarose beads from up to 800 μg of protein from control or FHKD adipocytes, respectively. Immunoblotting for 2SC confirms intense Keap1 succination, despite less total Keap1 immunoprecipitated from the FHKD lysates (Keap1/V5 panels). (C) Mass spectrum showing the regulatory Cys288 of Keap1 is modified by fumarate in the FHKD adipocytes (upper spectrum). The pyridyethylated form of this peptide was also detected (lower spectrum). (D-E) Immunoblotting was performed to detect ChOp and heme oxygenase 1 (HOX1) levels in 30 μg protein lysates from adipocytes matured in normal glucose and treated with 40 μM sulforaphane, 300 μM dimethylfumarate (DMF) or 10 μM MG132. Representative immunoblot from samples prepared with a minimum of n=3 per group. Coomassie blue staining indicates equal protein loading.

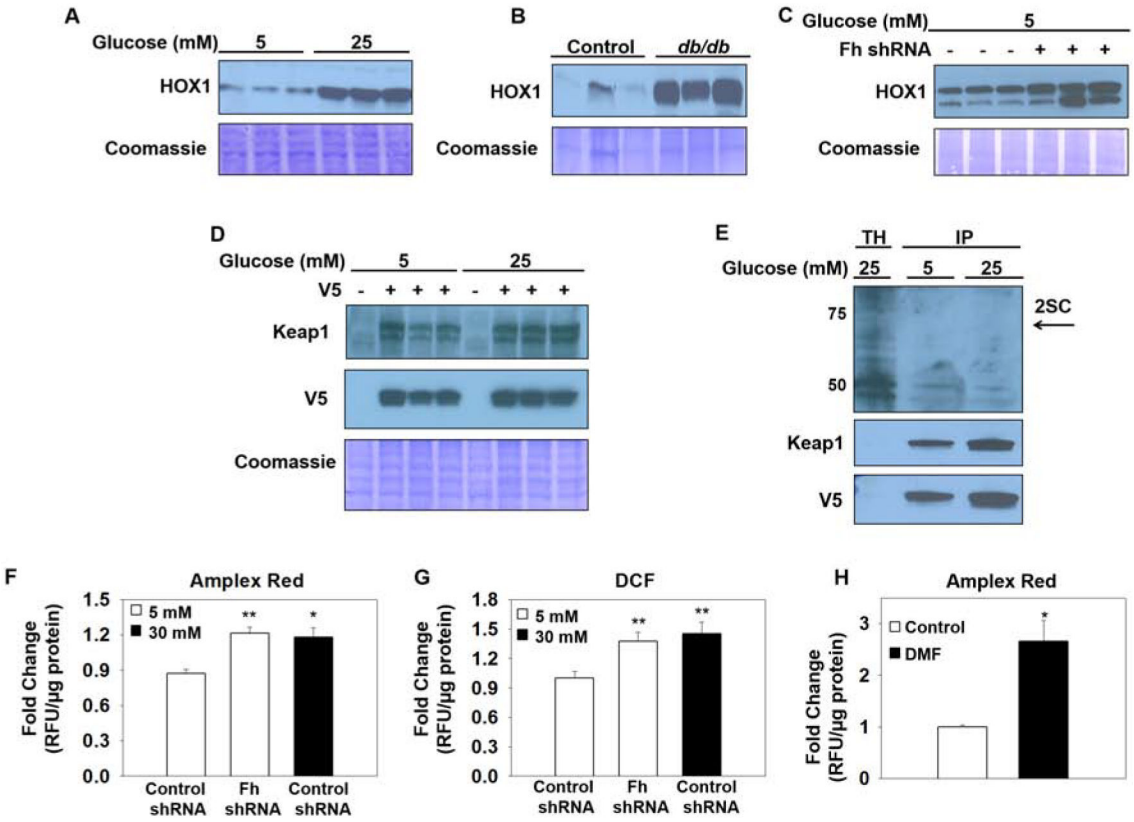

Figure 3: Fumarate augments oxidative stress to modify Keap1 and stabilize CHOP

(A-C) Protein from mature 3T3-L1 adipocytes, control or *db/db* epididymal adipose tissue and control or FHKD adipocytes was immunoblotted and probed to detect heme oxygenase 1 (HOX1) protein levels. (D) Immunoblotting with anti-Keap1 and -V5 antibodies validates the successful transduction of the scrambled control or Keap1-V5 tagged lentivirus in adipocytes matured in 5 mM or 25 mM glucose. (E) Protein (600 µg) from adipocytes matured in 5 mM or 25 mM glucose was immunoprecipitated with anti-V5 agarose beads. The eluted protein was immunoblotted to detect succination (2SC) in the the total homogenate (TH) and immunoprecipitate (IP), followed by re-probing with anti-Keap1 and -V5 antibodies. Arrow indicates anticipated position of succinated Keap1 (F-G) Measurement of reactive oxygen species was performed using both Amplex Red and DCF detection methods. Control or FHKD adipocytes were cultured in 5 or 30 mM glucose, or (H) 5 mM glucose and treated with 200 pM DMF (representative experiments shown with minimum n=3/group, mean +/− SEM, *p< 0.05, **p<0.001).

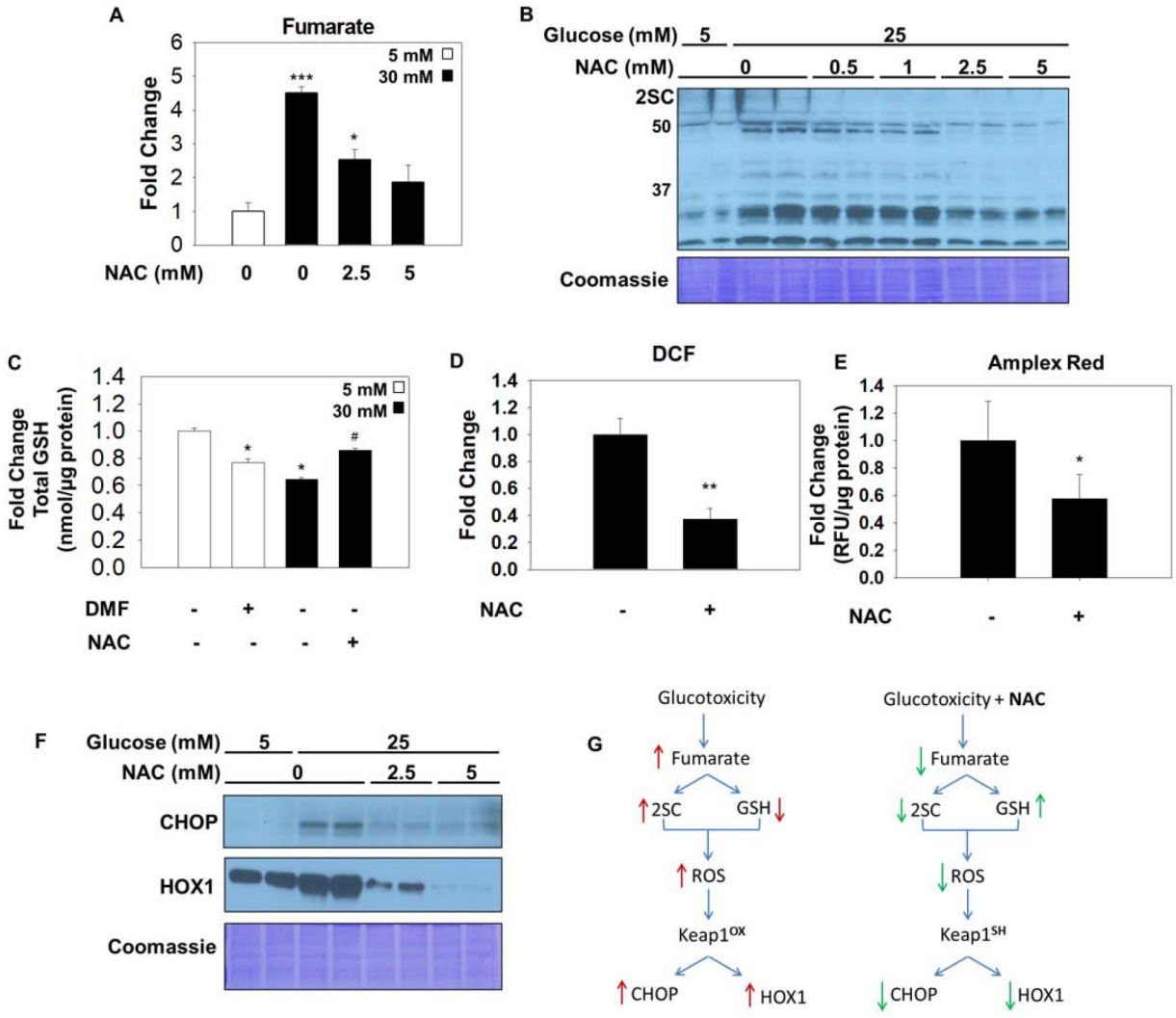

Figure 4: N-acetylcysteine reduces fumarate, protein succination and ROS

(A) Metabolites were extracted from adipocytes matured in 5 or 25 mM glucose, or 25 mM glucose treated with 5 mM NAC for 3 days. Fumarate levels are significantly increased with glucotoxicity and return to normal with NAC treatment. Data is normalized to total protein content (µg) (n=3/group, mean +/− SEM, *p< 0.05, ***p<0.001 vs. 5 mM glucose, $^{\#\#}$p<0.01 vs. 30 mM glucose). (B) 30 µg of protein from adipocytes cultured in 5 or 25 mM glucose and treated with 0, 0.5, 1, 2.5 or 5 mM N-acetylcysteine (NAC) for 8 days was immunoblotted to detect 2SC levels. (C) (D) Adipocytes were treated with 100 µM dimethyl fumarate (DMF) for 24 hours, or 5 mM NAC for 8 days. Total glutathione levels were quantified (n=3/group, mean +/− SEM, *p< 0.05 vs. 5 mM glucose, $^{\#}$p<0.05 vs. 30 mM glucose). Reactive oxygen species was measured using dichlorofluorescein in adipocytes matured in 30 mM glucose with or without 1 mM NAC for 8 hours (n=4/group, mean +/− SEM, **p<0.01). (E) CHOP and HOX1 levels were measured in adipocytes treated with 2.5 or 5 mM NAC for 8 days. Coomassie staining represents equal protein loading. (F) Schematic summarizing beneficial effect of N-acetylcysteine during glucotoxicity. Elevated glucose increases fumarate levels resulting in protein succination, reduced glutathione

(GSH) concentrations, and exacerbates the levels of reactive oxygen species (ROS) that react with redox-sensitive cysteines on Keap1. Oxidized Keap1 is unable unable to form the CSN supercomplex or to sequester Nrf2, resulting in the accumulation of CHOP and increased production HOX1. During high glucose stress N-acetylcysteine (NAC) decreases fumarate concentrations and protein succination and rescues the concentration of GSH in the adipocyte resulting in decreased ROS levels. In the absence of oxidative stress Keap1 is able to promote CHOP degradation and down regulate HOX1 production by sequestering Nrf2 in the cytosol.

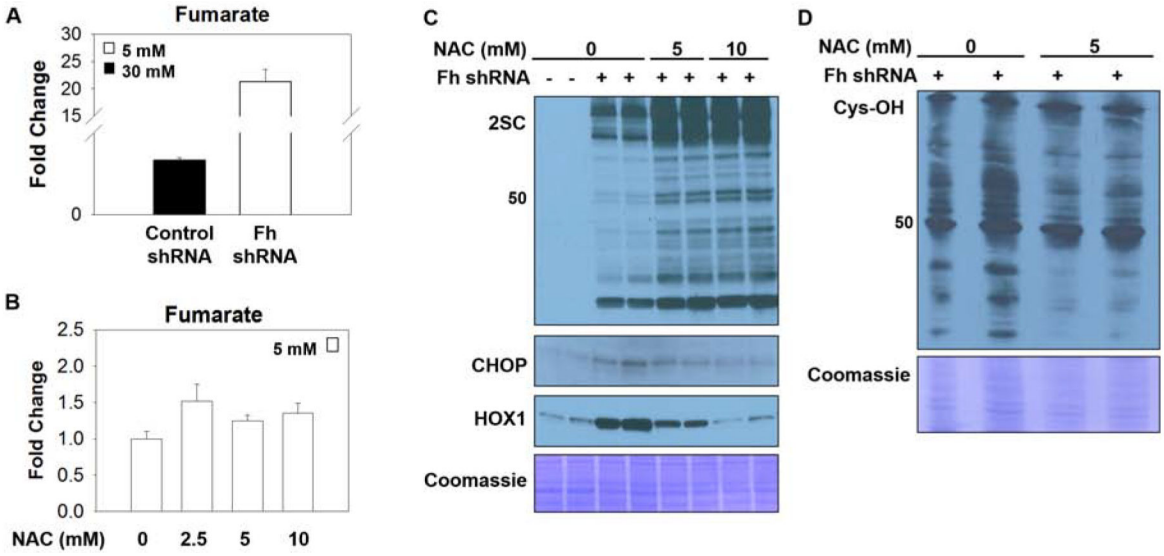

Figure 5: Protein oxidation regulates CHOP stability

(A) Fumarate levels were measured by GC-MS/MS following metabolite extraction from adipocytes matured 30 mM glucose or FHKD adipocytes in 5 mM glucose or (B) FHKD adipocytes cultured in 5 mM glucose and treated with 0, 2.5, 5 or 10 mM NAC for 3 days. Fumarate levels are normalized to total protein content of the samples. (C) Levels of 2SC, CHOP and HOX-1 were measured in control of FHKD adipocytes treated with 5 or 10 mM N-acetylcysteine (NAC) (D) Dimedone based detection of cysteine sulfenic acids was performed in lysates from FHKD adipocytes following treatment with NAC. Representative immunoblots shown, Coomassie indicates protein loading.

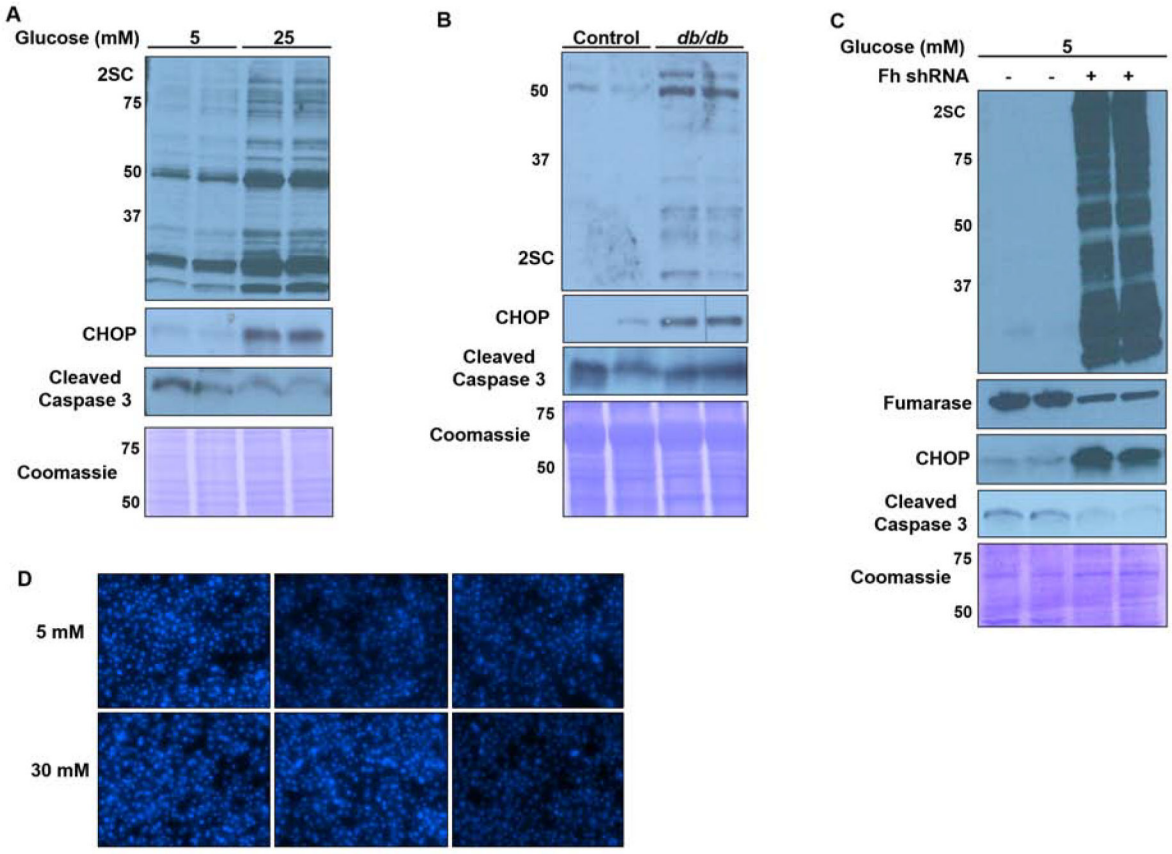

Figure 6: 2SC and CHOP accumulate in the absence of apoptosis

2SC and CHOP increase in parallel in (A) 3T3-L1 adipocytes, (B) 15 week old heterozygote control or *db/db* epididymal adipose tissue or (C) control or FHKD adipocytes, without an increase in the levels of cleaved caspase 3. Equal protein loading was confirmed by Coomassie. (D) Triplicate DAPI staining of nuclear content 5 mM or 30 mM glucose adipocytes matured for 8 days confirms no significant cell loss or evidence of apoptosis.

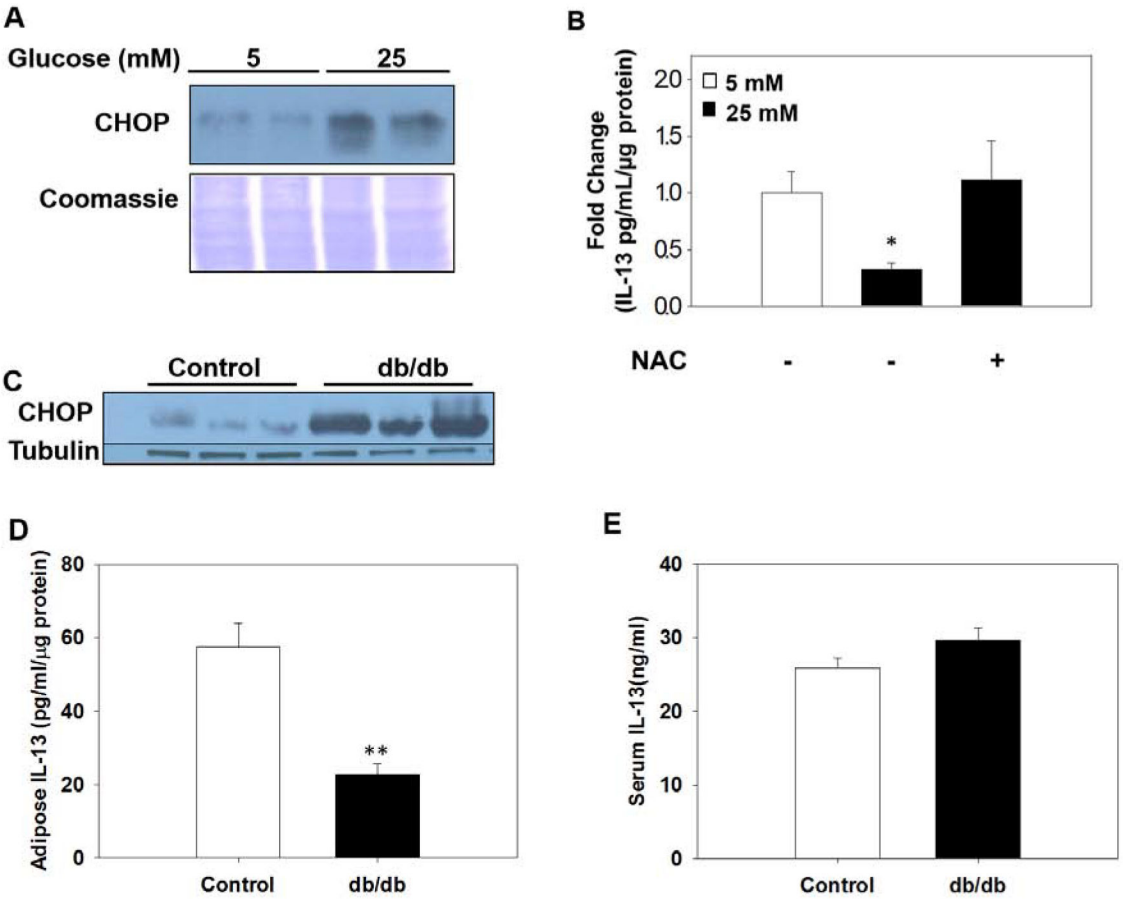

Figure 7: Accumulation of nuclear CHOP is associated with impaired IL-13 secretion by adipocytes

(A) The nuclear fraction from adipocytes cultured in 5 or 25 mM glucose demonstrates elevated nuclear CHOP levels during glucotoxicity. (B) Serum free conditioned medium was collected from adipocytes matured in normal or high glucose +/− 5 mM NAC and IL-13 levels were quantified (n=3/group, mean +/− SEM, *p< 0.05). (C) Confirmation of elevated CHOP protein levels in adipose tissue of 15 week old db/db (n=3 representative), in which IL-13 was quantified in (D) adipose tissue, p=0.004** and (E) serum, n=5 controls, n=6 db/db mice per group for the IL-13 quantification, normalized to protein levels.